# Quasielastic light scattering from rutile



doi: 10.1103/PhysRevB.60.12730

# Quasielastic light scattering from rutile

A. Koreeda, M. Yoshizawa, and S. Saikan
*Department of Physics, Graduate School of Science, Tohoku University, Sendai, 980-8578, Japan*

M. Grimsditch
*Materials Science Division, Argonne National Laboratory, Argonne, Illinois 60439*
(Received 9 February 1999; revised manuscript received 3 August 1999)

Quasielastic light scattering consisting of two components has been observed in single crystals of rutile ($TiO_2$). The broad component with a linewidth of 330 GHz at 297 K becomes narrower with decreasing temperature. In contrast, the narrow component, which has a linewidth of 1.1 GHz at 297 K, broadens as the temperature decreases. We present a unified explanation for both components, which is based on two-phonon difference Raman scattering. For the narrow component, it will be shown that two-phonon difference processes from a *single* acoustic phonon branch explain the temperature dependence of the intensity and the wave vector dependence of the linewidth at low temperatures. The conventional explanation in terms of entropy-fluctuation scattering is also attempted for temperatures above 200 K where phonon collisions occur more frequently than at lower temperatures and the phonon system may be considered hydrodynamically. For the broad component, two-phonon difference scattering from *different* phonon branches will be shown to provide a good explanation for the temperature dependent intensity. Furthermore, temperature dependence of the linewidth and its insensitivity to changes in scattering wave vector are also explained with this model. [S0163-1829(99)02642-9]

## I. INTRODUCTION

Low frequency light scattering has been a very useful method for studying the fundamental elastic and thermodynamic properties of crystals. Brillouin scattering, which has been most widely employed in this field, is the inelastic scattering of light by thermally excited acoustic phonons or other elementary excitations. In most Brillouin scattering experiments, the main interest has been the frequency shift, the intensity, and the linewidth of the Brillouin lines. Thus, less attention has been given to the lower frequency region or to the central component. This is primarily due to the difficulty in rejecting the usually intense, parasitically scattered, unshifted light.

Quasielastic light scattering consisting of two components was observed for the first time by Lyons and Fleury for the crystals of $KTaO_3$ and $SrTiO_3$.[1] They reported that the narrower component had a linewidth which was consistent with entropy-fluctuation scattering, which gives rise to a Lorentzian line profile with a half width of $D_{\rm th}Q^2/2\pi$, where $D_{\rm th}$ and $Q$ are the thermal diffusion constant and the wave vector transfer in the scattering experiment, respectively. In addition, the intensity of this component could not be explained by the usual Landau-Placzek theory, but was consistent with that predicted by Wehner and Klein,[2] who modified the theory of entropy-fluctuation scattering in crystalline solids. In Ref. 1, they also reported that the linewidth of the narrow component depends on $Q^2$, which was consistent with their assignment. However, the experimental results do not seem to be accurate enough to determine the exact power of $Q$. The broader component in their experiment was tentatively explained as arising from two-phonon difference Raman processes on the same acoustic phonon branch. In this paper we will show that the two-phonon difference process from a single acoustic phonon branch cannot scatter light with a frequency shift larger than the Brillouin component and hence cannot account for the broad component.

This type of light scattering has also been reported for diamond,[3] where a temperature induced line narrowing and $Q$-dependent linewidth were observed for the narrower quasielastic component. Entropy fluctuations are able to account for the linewidth of the narrow component at high temperatures, but do not reproduce the observed results at low temperatures. Two-phonon difference processes in the collision-free regime were then adopted to explain the characteristics of the narrow component at low temperatures. The broad component, whose linewidth did not depend on $Q$, was also ascribed to two-phonon difference processes.

Although two-phonon difference processes have long been proposed to explain the quasielastic light scattering in crystalline solids,[1,3–6] no explicit comparison between theory and experiment seems to have been made so far. A lack of experimental data is one of the reasons that such a comparison has not been made. In this paper, we report quasielastic light scattering from rutile ($TiO_2$) single crystals. The spectra have been found to consist of two components, which have characteristic temperature and wave vector dependences. We also present a unified physical interpretation for both components which is based on the two-phonon difference Raman processes. It will be shown that our explanation accounts for all the observed behavior at least qualitatively and in some case even quantitatively. A conventional analysis based on thermodynamic theory[2] is also presented for the narrow component.

## II. EXPERIMENT

Rutile has a tetragonal structure whose space group is $D_{4h}$ or $P4/mmm$. The refractive indices for ordinary and extraordinary rays at 514.5 nm are 2.69 and 3.01, respectively.[7] The

 

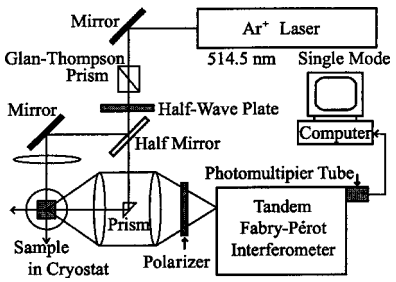


FIG. 1. Experimental setup for backscattering and right-angle scattering. The light source employed was an $Ar^+$ laser operated at a single longitudinal mode of 514.5 nm and the incident power was about 120 mW.

sample used for most of the experiments was an oriented single crystal with dimensions of $5\times5\times5$ mm$^3$, whose surfaces normal to the *a* and *c* axes were polished. We also used another sample in a shape of half cylinder whose diameter and height were 10 mm and 5 mm, respectively. The *c* axis of this sample was along the cylinder axis. The experimental setup is depicted in Fig. 1. The light source employed was an $Ar^+$ laser operated at a single longitudinal mode of 514.5 nm and the incident power was about 120 mW. The spectra were obtained with a Sandercock-type tandem Fabry-Pérot interferometer. The data acquisition time for each spectrum was about 30 and 60 min for backscattering and 90° scattering, respectively, at the scanning speed of 0.7 msec/channel for 512 channels.

## III. EXPERIMENTAL RESULTS

We have observed quasielastic light scattering consisting of two components in both our rutile samples. Figure 2 is a log-log plot of the observed spectrum at 297 K. The direction of **Q** was approximately parallel to the crystalline [100] direction and both the incident and the scattered light polarizations were parallel to the crystalline *c* axis. Other directions of **Q** gave similar results with slightly different linewidth in each case. The solid line represents the numerical fitting of a function consisting of two unshifted Lorentzians. The two quasielastic components exhibit different temperature dependences; at relatively high temperatures, the broad component is dominant, while at low temperatures only the narrow one is seen. This result is in contrast to the previous report on diamond,[3] where it was the narrow component that was dominant at high temperatures. In the following subsections we present the experimental results of each component in detail.

### A. The narrow quasielastic component

The temperature dependence of the narrow quasielastic component is shown in Fig. 3, which clearly exhibits the line narrowing as temperature increases. The dots are the experimental spectra and the solid lines are numerically fitted Lorentzian curves. The spectra were obtained in the backscattering geometry, where both incident and scattered light polarizations were parallel to the crystalline *c* axis. The wavevector transfer **Q** was along the crystalline [110] direction and $Q=7.34\times10^5$ cm$^{-1}$. In all the spectra in Fig. 3, the two pairs of shifted narrow lines labeled LA and TA are the

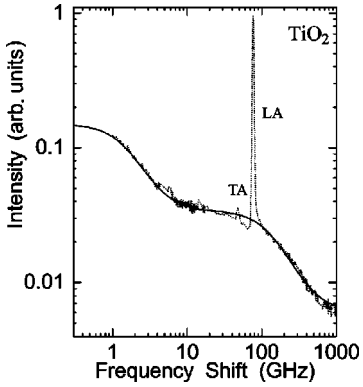


FIG. 2. Log-log plot of the observed spectrum of rutile at 297 K in the frequency range from 0.3 to 1000 GHz. The dotted line is the experimental data, which shows the well-resolved narrow and broad quasielastic scattering components and the longitudinal (LA) and transverse (TA) acoustic phonons, respectively. The direction of **Q** was approximately parallel to the crystalline [100] direction and both the incident and the scattered light polarizations were parallel to the crystalline *c* axis. The solid line represents the numerical fitting of a function consisting of two unshifted Lorentzians. Note that the spectrum is normalized at the peak height of the LA-Brillouin line. These data are a composite of several spectra which were obtained with different free-spectral ranges of the interferometer.

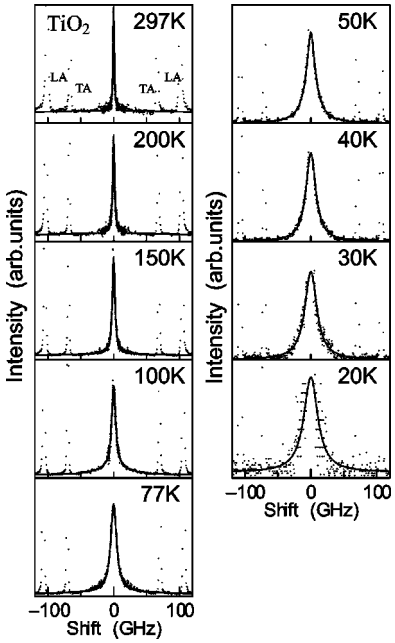


FIG. 3. Temperature dependence of the narrow quasielastic component in the temperature range from 20 to 297 K. The dotted lines are the measured spectra and the solid lines are numerically fitted Lorentzian curves. The two pairs of shifted narrow lines labeled LA and TA are the Brillouin lines of longitudinal and transverse acoustic phonons. The peak intensities of these lines are much higher than those of the central quasielastic component at all temperatures. The spectra were obtained with $\mathbf{Q}\|[110]$ and $Q=7.34\times10^5$ cm$^{-1}$. Note that the peak heights of these spectra have been normalized at each temperature.

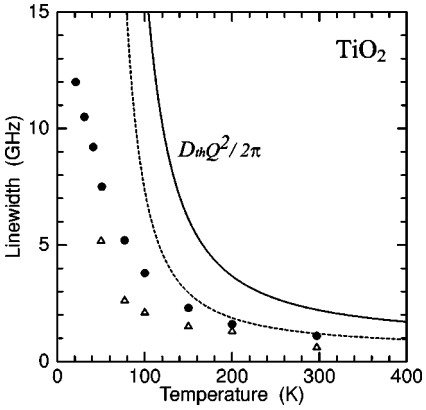


FIG. 4. Temperature dependence of the half width at half maximum of the narrow quasielastic component. The filled circles and the triangles are the measured linewidths for 180° and 90° scattering, respectively. The solid and broken lines represent the theoretical linewidth $D_{\mathrm{th}}Q^2/2\pi$ for backscattering and 90° scattering geometries, respectively.

longitudinal and transverse acoustic Brillouin lines, respectively. Note that, as for Fig. 2, the spectra in Fig. 3 are constructed by linking several spectra obtained with different free-spectral ranges. For clarity, the spectra are displayed with their peak heights normalized. The temperature dependence of the integrated intensity, which decreases with decreasing temperature, will be discussed later.

The half width at half maximum of the narrow component, determined by the Lorentzian fitting, depends on temperature as shown in Fig. 4. The filled circles and the triangles are the experimentally measured linewidths obtained in backscattering and 90° scattering, respectively. The direction of **Q** was along [110] in both scattering geometries and the magnitudes of **Q** were $7.34\times10^5$ cm$^{-1}$ and $5.19\times10^5$ cm$^{-1}$ for backscattering and 90° scattering, respectively. It can be seen that the linewidth depends rather strongly on temperature at low temperatures, while at high temperatures its dependence on temperature becomes weaker. The solid and broken lines represent the linewidths which are calculated from thermodynamic theory, which predicts an unshifted Lorentzian line shape with linewidth of $D_{\mathrm{th}}Q^2/2\pi$, where $D_{\mathrm{th}}$ is thermal diffusion constant. We estimated $D_{\mathrm{th}}$ from the well-known relation $D_{\mathrm{th}}=\kappa/\rho C_p$, where $\kappa$, $\rho$, and $C_p$ are thermal conductivity[8] and density and specific heat under constant pressure,[9] respectively. At low temperatures, the calculated linewidths are much broader than those observed for both values of $Q$. Furthermore, even at the highest temperature of 300 K, the calculated values are about twice as broad as those observed. We also see in Fig. 4 that the linewidth of the narrow component depends on the magnitude of the wave vector transfer. The signal intensity in the 90° scattering experiment, however, was not strong enough to allow an accurate wave vector dependence of the narrow component linewidth.

The behavior described above is similar to that found in diamond,[3] where the temperatures were much higher and the observed linewidths were larger than those in rutile. At the highest temperature of about 1200 K the widths for 90° scattering and 34° scattering were about 12 and 2 GHz, respectively, which were quantitatively consistent with $D_{\mathrm{th}}Q^2/2\pi$

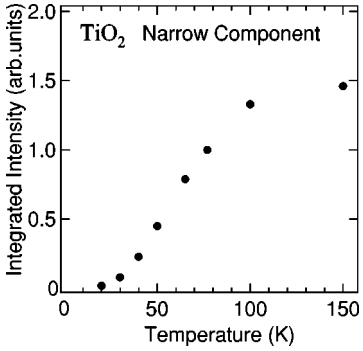


FIG. 5. Temperature dependence of the narrow component integrated intensity normalized at 77 K for later discussion. The integrated intensity increases with temperature as to $T^3$ below 50 K, it rather slowly increases above 50 K.

for diamond. Since they found that the intensity ratio of the narrow central component to the Brillouin component was also in good agreement with the modified Landau-Placzek ratio of Wehner and Klein,[2] they concluded that the narrower component at high temperature was due to entropy fluctuations. It must be noted that the phonon mean-free path must be sufficiently short compared to $Q^{-1}$ in order for hydrodynamic picture to be valid. In the opposite limit, i.e., very long phonon mean-free paths, one must consider that the light is scattered by individual phonons rather than by collective excitations such as diffusing heat.[10] Reviewing Fig. 4, it is obvious that we should not apply thermal diffusion theory to the low temperature data. In fact, the phonon mean-free path of rutile is estimated to be of the same order of or longer than $Q^{-1}$ at temperatures lower than 150 K, which indicates a nonhydrodynamic regime.[3]

The integrated intensity of the narrow component depends on temperature as shown in Fig. 5. It increases rapidly with temperature below 50 K, is roughly linear between 50 and 100 K, and then seems to reach a plateau above 100 K. According to the above arguments regarding the hydrodynamic and nonhydrodynamic regimes, the different temperature regions seem to correspond to the two scattering regimes: the narrow component in the lower temperature region corresponds to two-phonon difference scattering and that in the higher temperature region can be considered to be due to entropy fluctuations. However, since the observed linewidth was narrower than $D_{\mathrm{th}}Q^2/2\pi$ even at 300 K, it implies that 300 K is still too low for the present system to be considered fully hydrodynamically. Therefore, it might be more appropriate that we consider the temperature region around 300 K in our experiment as an intermediate regime between hydrodynamic and nonhydrodynamic. The low temperature data of the integrated intensity will be discussed in the following section from the viewpoint of two-phonon difference scattering.

### B. The broad quasielastic component

The temperature dependence of the broad quasielastic component is shown in Fig. 6, where the spectra are numerically fitted by Lorentzian functions and displayed with their peak height normalized again. The Brillouin components due to the longitudinal acoustic phonons appear as sharp peaks

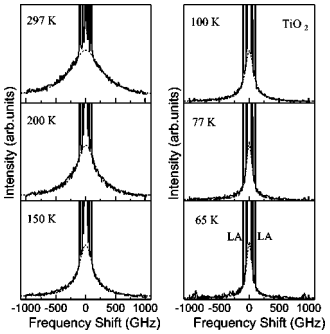


FIG. 6. Temperature dependence of the broad quasielastic component. The dashed lines are the numerically fitted Lorentzians. The sharp peaks appearing near the center of the spectra are the Brillouin components due to longitudinal acoustic phonons.

near the center of the spectra. The narrow component, described in the previous subsection, is not resolved and it appears as the elastic peak. Although the broad quasielastic component is strong in the spectra at high temperatures, its integrated intensity and linewidth (half width at half maximum) decrease with decreasing temperature as indicated in Figs. 7 and 8; it becomes undiscernible below 65 K. These temperature dependences will be discussed and explained in the following section.

This broad component has little wave vector dependence as shown in Fig. 9. The linewidths in Figs. 9(a) and 9(b) are 303 and 313 GHz, respectively. Note that the frequency shifts of the Brillouin lines differ in the two spectra according to their linear $Q$ dependence.

## IV. DISCUSSION

In this section we present an explanation for our observation, which is based on two-phonon difference Raman processes. We argue that two-phonon difference processes from a single phonon branch account for the narrow quasielastic component, while two-phonon difference processes from different phonon branches explain the broad quasielastic component.

### A. The narrow quasielastic component

The model used here to describe second order difference Raman scattering involves two important approximations: it

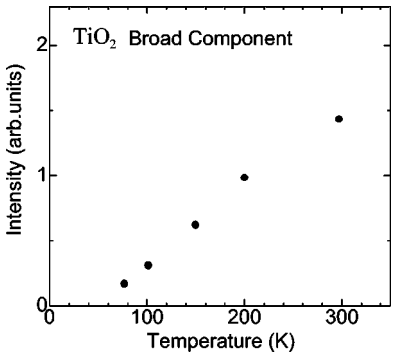


FIG. 7. Temperature dependence of the integrated intensity of the broad quasielastic component. The values are normalized at 200 K for later convenience.

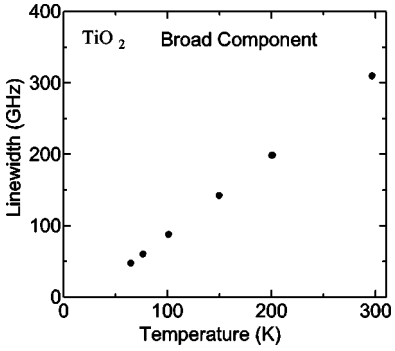


FIG. 8. Temperature dependence of the half width at half maximum of the broad quasielastic component. The widths were determined from Lorentzian fitting to the measured spectra. The narrowest width is about ten times as broad as the width of the narrow component at the same temperature.

assumes an isotropic phonon dispersion and also that the Raman matrix elements are independent of the initial and final states. In spite of these simplifications, we will show that the model provides an excellent explanation of our observations.

Consider an isotropic phonon branch $\omega(k)$, where $k$ is the magnitude of the wave vector $\mathbf{k}$. In a first order Raman process, we create an excitation with wave vector $\mathbf{Q}$. If we assume an acoustic branch and take $Q$ to be small, the frequency shift corresponding to the Brillouin component is $\omega_B = Q[\partial\omega(k)/\partial k]|_{k=0} = Qv$, where $v$ is the sound velocity. In a two-phonon difference Raman process, an excitation with wave vector $\mathbf{k}$ is annihilated and another with wave vector $\mathbf{k}+\mathbf{Q}$ is created. In the approximation of an isotropic solid, the change in frequency associated with this process depends only on the projected component of $\mathbf{Q}$ onto $\mathbf{k}$,

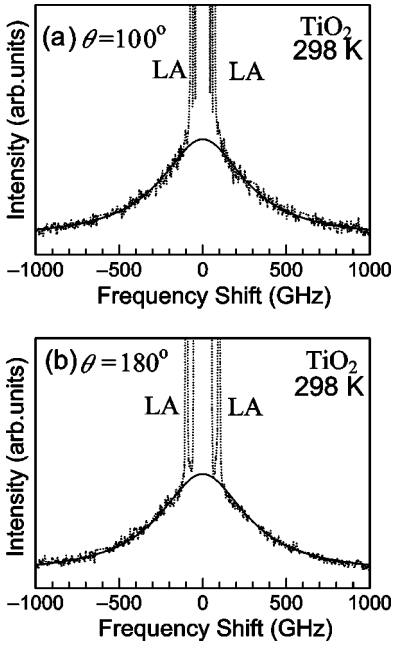


FIG. 9. The wave vector ($Q$) dependence of the broad quasielastic component. The measured linewidths were, respectively, 303 GHz in (a) with the scattering angle of 100°, and 313 GHz in (b) with the scattering angle of 180°.

which can be written as $Q\cos\theta$, where $\theta$ is the angle between **Q** and **k**. The two-phonon difference process gives rise to a frequency shift $\Omega$ as

$$\Omega = \omega(k + Q\cos\theta) - \omega(k) = \frac{\partial\omega(k)}{\partial k} Q\cos\theta. \quad (1)$$

The entire two-phonon difference Raman spectrum is the sum of contributions from all the allowed values of $k$ and $\theta$ which satisfy Eq. (1). For fixed values of $k$ and $\theta$, the intensity at frequency shift $\Omega$ can be written as

$$I(\Omega,k)dkd\theta \propto 2\pi k^2 \sin\theta\,\delta\left(\theta - \arccos\frac{\Omega}{Q[\partial\omega(k)/\partial k]}\right)dkd\theta, \quad (2)$$

where the delta function is introduced to include the restriction for $k$ and $\theta$ due to Eq. (1). On integrating Eq. (2) over $\theta$, we obtain

$$I(\Omega,k)dk \propto 2\pi k^2 \sqrt{1-\left(\frac{\Omega}{Q[\partial\omega(k)/\partial k]}\right)^2}\,dk. \quad (3)$$

Now we incorporate the thermal population factor of the relevant phonons. For the two-phonon difference process with which we are concerned, it is given by

$$n(\mathbf{k})[n(\mathbf{k}+\mathbf{Q})+1] \approx n(k)[n(k)+1],$$

where the Bose-Einstein factor is defined as $n(k) = \{\exp[\hbar\omega(k)/k_BT]-1\}^{-1}$.

Noting that the integration must be performed over the values of $k$ which satisfy

$$1-\left(\frac{\Omega}{Q[\partial\omega(k)/\partial k]}\right)^2 \geqslant 0 \quad (4)$$

in order to avoid imaginary results, we obtain the total intensity as

$$I(\Omega) \propto \int_0^{\pi/a} dk\, n(k)[n(k)+1]k^2 \sqrt{1-\left(\frac{\Omega}{Q[\partial\omega(k)/\partial k]}\right)^2}, \quad (5)$$

where $a$ is the lattice constant. Normalizing $k$ and $\Omega$ as $\kappa = ka$ and $\Delta\Omega = \Omega/\omega_B$ leads to the following expression for the total intensity:

$$I(\Omega) \propto \int_0^{\pi} d\kappa\, n(\kappa)[n(\kappa)+1]\kappa^2 \sqrt{1-\left(\frac{\nu}{a}\frac{\Delta\Omega}{[\partial\omega(\kappa)/\partial\kappa]}\right)^2}. \quad (6)$$

Equation (6) predicts the line shape and intensity at any temperature $T$.

Figure 10 shows the temperature dependence of the calculated line shape of the narrow component. The peak intensities are normalized at each temperature. The line shape is in good agreement with the observation. Furthermore, the temperature induced spectral narrowing is also fairly well reproduced. The phonon dispersion $\omega(k)$ used for the calculation was taken as the lower TA branch, namely, $\Sigma_2(1)$ in the neutron scattering data of rutile.[11] Note, however, that we still assumed spherical symmetry for the dispersion curve. We chose $\Sigma_2(1)$ dispersion curve because it corresponds to our **Q** direction, viz., [110]. Other dispersion curves, such as the LA branch and a simple $\omega(k) = \omega_0\sin(ka/2)$ with $\omega_0$ equal to the zone boundary frequency, were also tested but produced slightly worse agreement. We did find that the calculated line shapes are critically affected by the shape of the dispersion curves indicating that the real anisotropic dispersion curves and the inclusion of all three acoustic branches would provide more exact predictions.

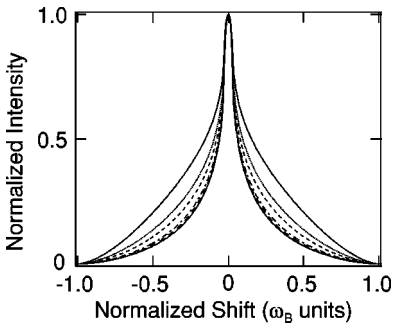


FIG. 10. Temperature dependence of the calculated line shape of the narrow quasielastic component. The broadest line is at 30 K, intermediate curves at 40, 50, 77, and 100 K, and the narrowest at 150 K. The isotropic dispersion curve which was used for the calculation was $\Sigma_2(1)$ in Ref. 11. Note that the horizontal axis is normalized by the Brillouin frequency $\omega_B$.

The calculated linewidth depends on temperature as shown in Fig. 11, where one should note that the linewidth is plotted in $\omega_B$ units. The observed linewidths which are normalized by $\omega_B$ are also plotted in Fig. 11. The Brillouin frequency which was used for normalization of the linewidths is 66 GHz, observed transverse acoustic phonon frequency. It can be seen from Fig. 11 that the $\Sigma_2(1)$-like dispersion curve yields consistent linewidths at low temperatures, but its predictions are too broad at higher temperatures. As mentioned above, since the linewidth is greatly influenced by the shape of the dispersion curve, more exact predictions may be obtained by taking the real anisotropic phonon dispersions into account.

The temperature dependence of the integrated intensity which was calculated from Eq. (6) with a dispersion curve

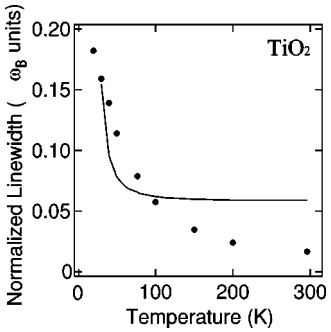


FIG. 11. Temperature dependence of the narrow component linewidth calculated using Eq. (6) (solid line). The dots are the observed widths which are normalized by the Brillouin frequency of 66 GHz, the observed transverse acoustic phonon frequency of rutile. At low temperatures, the calculated linewidth reproduces the observations better than $D_{\text{th}}Q^2/2\pi$.

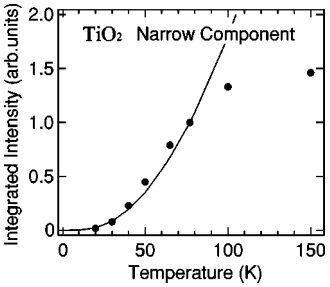


FIG. 12. Temperature dependence of the integrated intensity of the narrow component which was calculated from Eq. (6) with a dispersion curve $\Sigma_2(1)$; solid line represents the calculated result and the dots are the observed intensities. The values are normalized to 1 at 77 K.

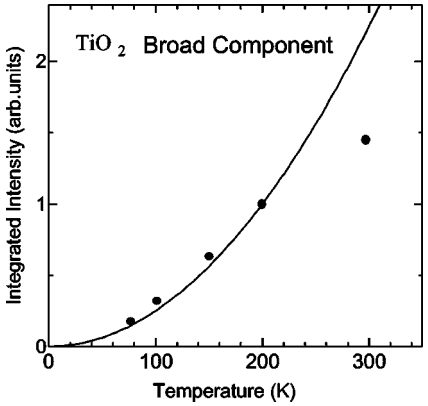


FIG. 13. Calculated temperature dependence of the integrated intensity of the broad component (line). The dots are the observed integrated intensity of the broad component. The values are normalized at 200 K for ease of comparison.

similar to $\Sigma_2(1)$ is displayed as a solid line in Fig. 12 together with the experimental integrated intensities (dots). In Fig. 12 both the observed and the calculated values are normalized at 77 K. A quantitative agreement is seen up to 100 K, above which the calculated values are too large. The calculated integrated intensity, which can be approximated as proportional to $T^2$ at high temperatures, deviates from the experimental results above 100 K.

Since the calculated linewidth scales as $\omega_B$, it is expected to be proportional to $Q$. This prediction is different from that of entropy fluctuations which predict a $Q^2$ dependence of the linewidth. In Ref. 3, the temperature and wave vector dependence of the narrow component linewidth of diamond are investigated and the authors concluded that, while entropy fluctuations account for the narrow component at high temperatures, deviations appeared at low temperatures. The ratio of the linewidths in Fig. 4 fall in the range $1.7 \pm 0.3$. This must be compared width 1.4 and 2.0 predicted by our model and the entropy-fluctuation model, respectively; clearly our accuracy is not sufficient to distinguish between the two models on this point. It is very interesting to note that the measured widths in diamond in Ref. 3 seem to scale as $Q$ at 700 K, which was relatively low temperature in their experiment, while it scales as $Q^2$ at the highest temperature.

### B. The broad quasielastic component

The broad quasielastic component can be explained by two-phonon difference processes from different phonon branches near the zone boundary. Consider two phonons on a pair of merging branches at a zone boundary point. We annihilate one phonon on one branch and create the other phonon on the other branch. The frequency shifts which are caused by this kind of phonon pairs give rise to central peak whose intensity is predicted by a factor $n(\omega_{\mathrm{ZB}})[n(\omega_{\mathrm{ZB}})+1]$, where $\omega_{\mathrm{ZB}}$ is the zone boundary frequency. For the lowest zone boundary points of rutile, $\omega_{\mathrm{ZB}}$ is approximately 3.1 THz.[11] Figure 13 is the plot of the calculated integrated intensity of the broad component with $\omega_{\mathrm{ZB}} \approx 3$ THz.

Since $Q$ is very small compared with $k_{\mathrm{ZB}}$, the two-phonon difference processes from different phonon branches are expected to cause little difference in the line shape of the broad component with respect to the change in $Q$. This is in good agreement with the experimental results shown in Fig. 9. Within the framework developed here it is not possible to obtain reliable values of the width of this broad quasielastic component. First, because the line shape depends on the nature of the critical point at the zone boundary and analytical expressions for these singularities contain divergences; it is, therefore, not possible to extract linewidths without incorporating techniques to circumvent the singularities. Second, even at the lowest temperatures, there are at least three different critical points that contribute.[11] Qualitatively, however, the linewidth of the broad component will be related to how steeply the branches diverge away from each other; a slow divergence producing a narrower line. The line shape due to each critical point is not expected to change with temperature. The experimentally observed temperature induced broadening, however, is consistent with the contributions from the higher frequency critical points at which the phonon branches diverge from each other more rapidly. These contributions, which only become activated at higher temperatures, produce a broader line.

## V. SUMMARY

Quasielastic light scattering consisting of two components was observed in single crystals of rutile. We experimentally clarified the temperature dependences of the linewidth and the intensity of both the narrow and the broad components. We also formulated an explanation based on two-phonon difference Raman processes for both components. The narrow component is well explained by two-phonon difference processes from a single acoustic phonon branch. With this model, the temperature dependence of the integrated intensity was consistent with our observations and the temperature induced line narrowing was reproduced qualitatively. At high temperatures, however, the narrow component may be better explained by entropy fluctuations since the observed linewidth approaches the values expected from thermal diffusion theory. Further experiments are necessary to distinguish the difference of the wave vector dependence between these two explanations, i.e., the difference between $Q$ and $Q^2$. The experimental results of the broad component were well explained by two-phonon difference processes from different phonon branches near the zone boundary. The temperature dependence of the integrated intensity of the broad component was found to follow $n(n+1)$, which is expected from the two-phonon difference Raman processes.

**ACKNOWLEDGMENTS**

We thank Dr. J. R. Sandercock for many fruitful discussions. This work has been supported by CREST of Japan Science and Technology Corporation (JST). Work at Argonne National Laboratory was supported by the U.S. Department of Energy BES Materials Sciences under Contract No. W-31-109-ENG-38.

[1] K.B. Lyons and P.A. Fleury, Phys. Rev. Lett. **37**, 161 (1976).
[2] R.K. Wehner and R. Klein, Physica (Utrecht) **62**, 161 (1972).
[3] H.E. Jackson, R.T. Harley, S.M. Lindsay, and M.W. Anderson, Phys. Rev. Lett. **54**, 459 (1985).
[4] M. W. Anderson, S. M. Lindsay, and R. T. Harley, J. Phys. C **17**, 6877 (1984).
[5] P. R. Stoddart and J. D. Comins, in *Proceedings of the Sixteenth International Conference on Raman Spectroscopy*, edited by A. M. Heyns (Wiley, Chichester, 1998), pp. 880-881.
[6] A. D. Bruce and R. A. Cowly, Adv. Phys. **29**, 219 (1980).
[7] J.R. DeVore, J. Opt. Soc. Am. **41**, 416 (1951).
[8] *Thermophysical Properties of Matter, The TPRC Data Series*, edited by Y. S. Touloukian (IFI/Plenum, New York, 1970), Vol. 2.
[9] *Thermophysical Properties of Matter, The TPRC Data Series*, edited by Y. S. Touloukian (IFI/Plenum, New York, 1970), Vol. 5.
[10] P.A. Fleury and K. B. Lyons, in *Light Scattering Near Phase Transitions*, edited by H. Z. Cummins and A. P. Levanyuk (North-Holland, Amsterdam, 1983).
[11] J.G. Traylor, H.G. Smith, R.M. Nicklow, and M.K. Wilkinson, Phys. Rev. B **3**, 3457 (1971).